Supporting Information

Black Rutile of $(Sn,Ti)O_2$ initializing electrochemically Reversible Sn Nanodots Embedded in Amorphous Lithiated Titania Matrix for Efficient Lithium Storage

Jijian Xu[1,2§], Wujie Dong[3§], Changsheng Song[1], Yufeng Tang[1], Wenli Zhao[1], Zhanglian Hong[2,], Fuqiang Huang[1,2,3,*]*

[1] State Key Laboratory of High Performance Ceramics and Superfine Microstructure, Shanghai Institute of Ceramics, Chinese Academy of Sciences, Shanghai 200050, P.R. China;

[2] State Key Laboratory of Silicon Materials, School of Materials Science and Engineering, Zhejiang University, Hangzhou 310027, P.R. China;

[3] State Key Laboratory of Rare Earth Materials Chemistry and Applications, College of Chemistry and Molecular Engineering, Peking University, Beijing 100871, P.R. China.

[§]These authors contributed equally to this work.

*Corresponding Author: huangfq@mail.sic.ac.cn; hong_zhanglian@zju.edu.cn

Theoretical Section

Calculations have been performed within the framework of density functional theory (DFT) as implemented by the Vienna an initio Simulation Package (VASP).[S1,S2] The exchange-correlation energy is treated in the generalized-gradient approximation (GGA) using Perdew-Burke-Ernzerhof (PBE) functional.[S3] The model was constructed on the 1×1 (101) surface (30 atomic layer) with a 20 Å vacuum layer. Here, the cutoff energy of plane wave was chosen at 450 eV. For the structure optimizations, 7×7×1 Monkhorst-Pack (MP) grids were used. The changes in total energies between two successive electronic steps are less than 10-5 eV, meanwhile, all the Hellmann-Feynman force acting on each atoms was lower than 0.05 eV /Å.

Table S1. Comparison of capacity retention and high rate performance for $(Sn,Ti)O_2$ based anodes.

$(Sn,Ti)O_2$-based systems	**Elemental ratio**	**Long cycles@0.2 A g^{-1} (mA h g^{-1})**	**High rate capacity (mA h g^{-1})**	**References**
Black $(Sn,Ti)O_2$	**80 at% Sn**	**583 (100 cycles)**	**335 (5 A g^{-1})**	**Our work**
SnO_2 nanoflakes on TiO_2 nanotubes	80 at% Sn	530 (50 cycles)	358 (3.2 A g^{-1})	2014 [S4]
SnO_2@TiO_2 double shell nanotubes	48 at% Sn	300 (50 cycles)	200 (1.5 A g^{-1})	2013 [S5]
$(Sn,Ti)O_2$ solid solution nanorods	20 at% Sn	300 (50 cycles)	217 (3 A g^{-1})	2013 [S6]
Ordered network of interconnected SnO_2	100 at% Sn	564 (100 cycles)	300 (4.7 A g^{-1})	2015 [S7]
Black anatase titania	100 at% Ti	188 (100 cycles)	158 (5 A g^{-1})	2013 [S8]

Table S2 Lattice parameters of the samples with different stoichiometric.

Sample	2-Theta(110)	$d_{(110)}$-calculated	$d_{(110)}$-theoretical
B-SnO_2	26.611	3.347	3.347
B-$S_{0.8}T_{0.2}O_2$	26.790	3.325	3.327
B-$S_{0.6}T_{0.4}O_2$	26.964	3.304	3.307
Rutile-TiO_2	27.446		3.247

Table S3 Comparison of the detail data of equivalent circuit for (Sn,Ti)O_2 based anodes.

Sample	R_s	R_{ct}	W-R	W-T	W-P	CPE-P	CPE-T
B-STO_2	3.89	90.1	119.9	0.9479	0.4497	0.7461	$2.761*10^{-5}$
W-STO_2	4.2	192.0	171.9	1.409	0.4488	0.7927	$1.536*10^{-5}$

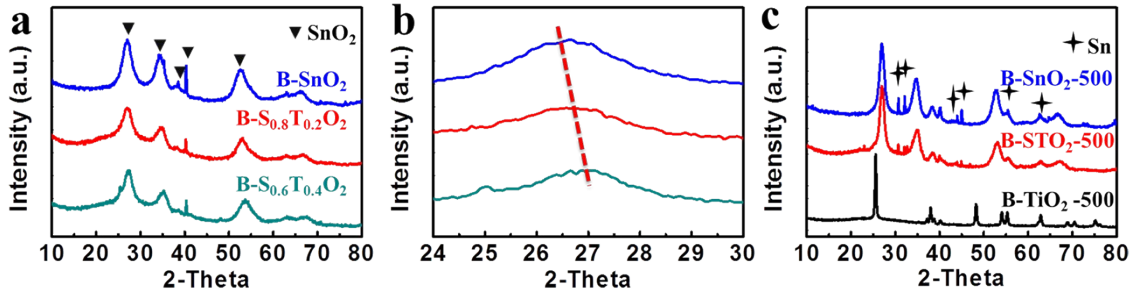

Figure S1. XRD characterization of the samples with different stoichiometric (a), partial magnifications of the region showing the shift of peak positions (b), and samples after hydrogen plasma reduction at 500 °C.

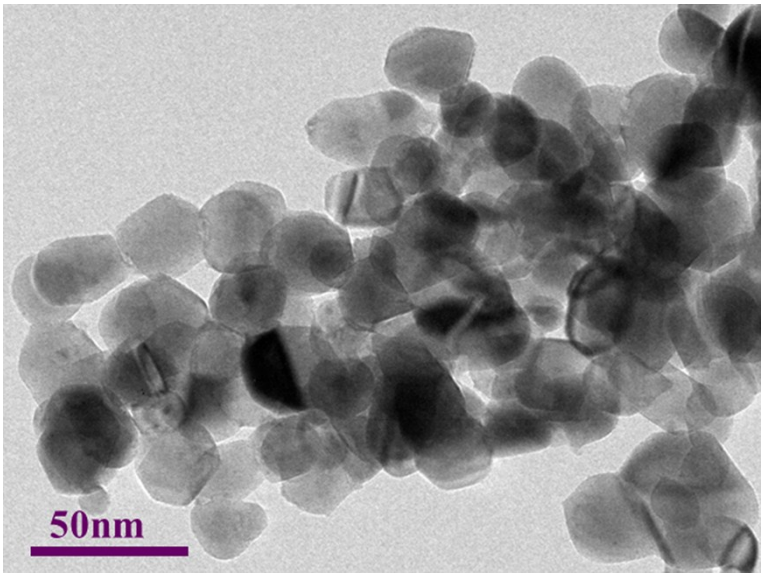

Figure S2. The TEM of air annealed W-STO_2.

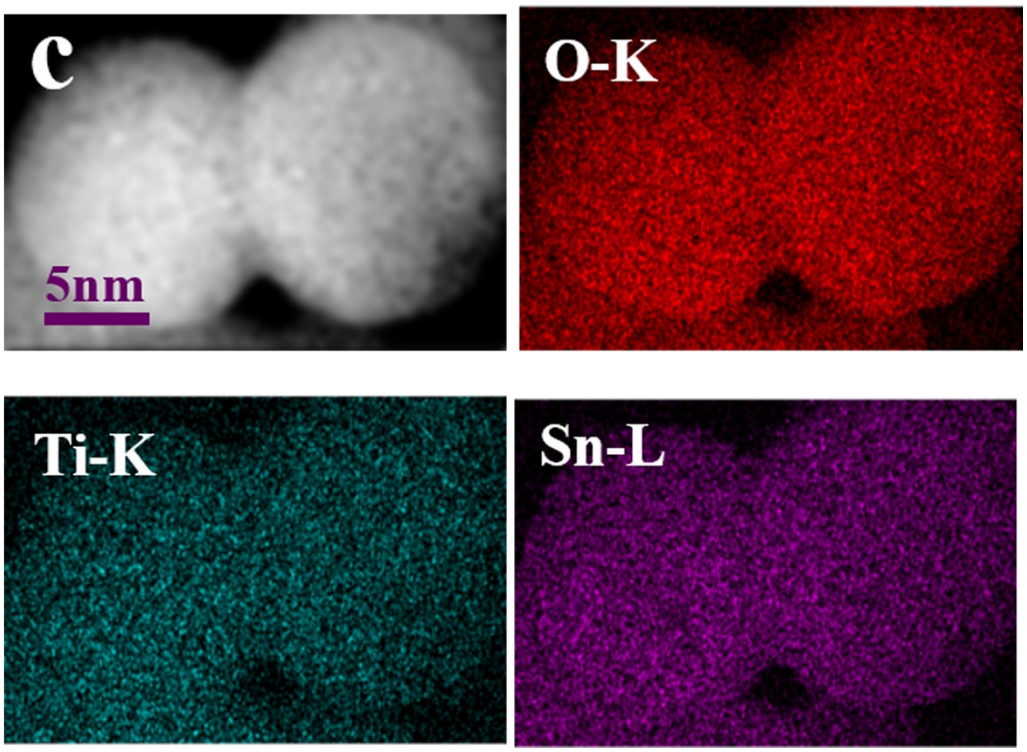

Figure S3. Elemental mapping images of B-STO_2 of oxygen, titanium, and stannum.

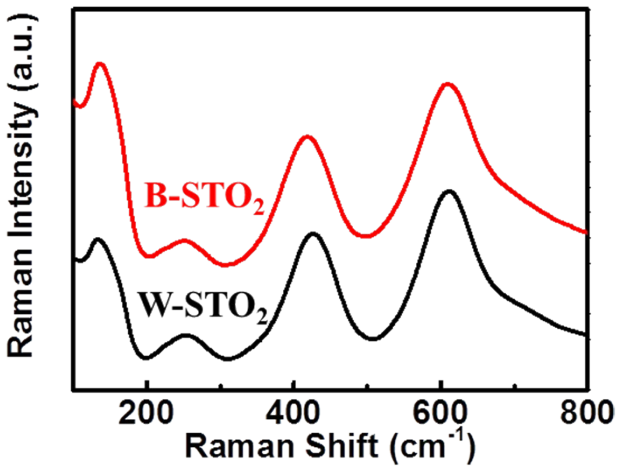

Figure S4. The Raman spectra of air annealed W-STO_2, and B-STO_2 after hydrogen plasma reduction.

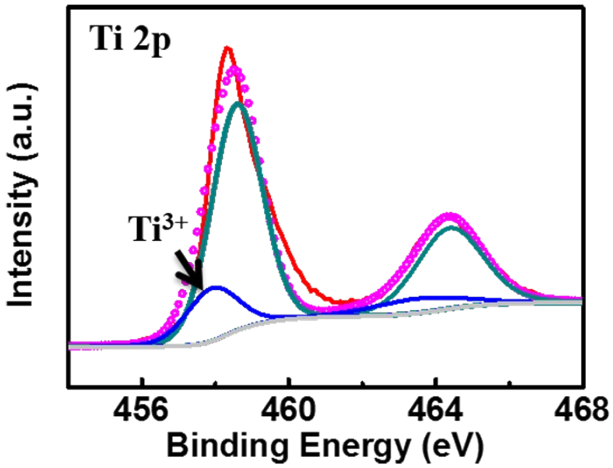

Figure S5. The XPS spectra of hydrogen plasma reduced B-STO_2.

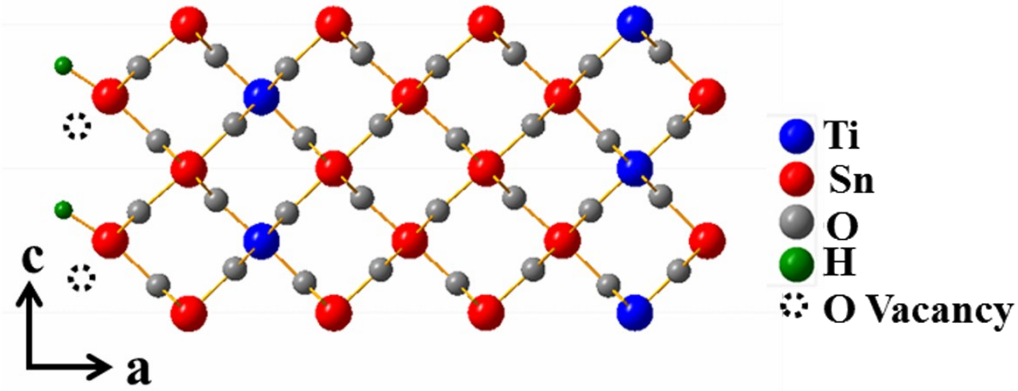

Figure S6. Schematic of the structure of B-STO_2.

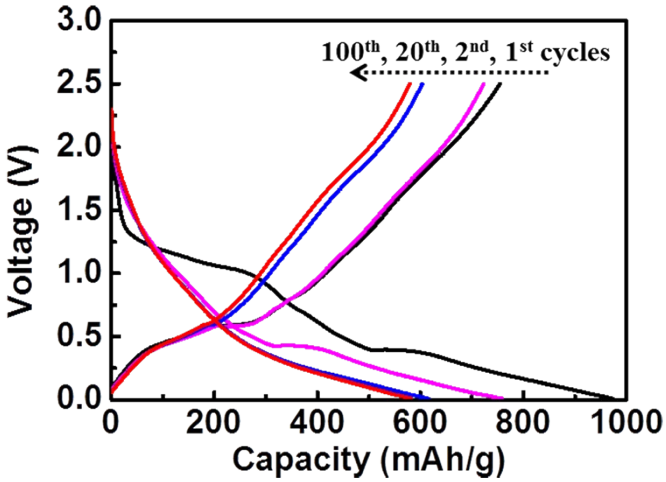

Figure S7. Galvanostatic charge/discharge curves of the 1st, 2nd, 20th, and 100th cycle of the B-STO_2 electrode.

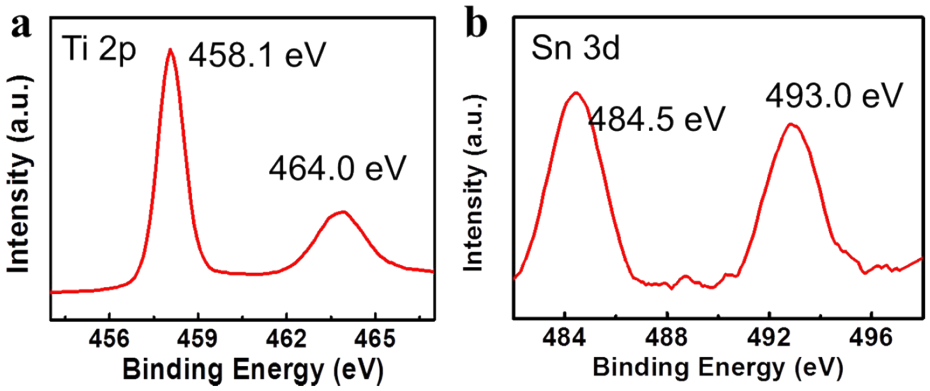

Figure S8. Sn 3*d* spectra and Ti 2*p* spectra of B-STO_2 after discharging.

[S1] P. E. Blöchl, *Phys. Rev. B* 1994, 50, 17953.

[S2] G. Kresse, and J. Furthmüller, *Phys. Rev. B* 1996, 54, 11169.

[S3] M. C. Payne, M. P. Teter, D. C. Allan, T. A. Arias, J. D. Joannopoulos, *Rev. Mod. Phys.* 1992, 64, 1045.

[S4] C. R. Zhu, X. H. Xia, J. L. Liu, Z. X. Fan, D. L. Chao, H. Zhang, H. J. Fan, *Nano Energy* 2014, 4, 105.

[S5] J. H. Jeun, K. Y. Park, D. H. Kim, W. S. Kim, H. C. Kim, B. S. Lee, H. Kim, W. R. Yu, K. Kang, S. H. Hong, *Nanoscale*, 2013, 5, 8480.

[S6] C. C. Chang, Y. C. Chen, C. W. Huang, Y. H. Su, C. C. Hu, *Electrochim. Acta* 2013, 99, 69.

[S7] V. Etacheri, G. A. Seisenbaeva, J. Caruthers, G. Daniel, J. M. Nedelec, V. G. Kessler, V. G. Poi, *Adv. Energy Mater.* 2015, 5(5).

[S9] S. T. Myung, M. Kikuchi, C. S. Yoon, H. Yashiro, S. J. Kim, Y. K. Sun, B. Scroasti, *Energy Environ. Sci.* 2013, 6, 2609.